

Fluid Line Evacuation and Freezing Experiments for Digital Radiator Concept

Daniel F. Berisford¹, Gajanana C. Birur², Jennifer R. Miller³, Eric T. Sunada⁴, Gani B. Ganapathi⁵
Jet Propulsion Laboratory, California Institute of Technology, Pasadena, CA

Ryan Stephan⁶
NASA Johnson Space Center, Houston, TX

Mark Johnson⁷
Boise State University, Boise, ID

The digital radiator technology is one of three variable heat rejection technologies being investigated for future human-rated NASA missions. The digital radiator concept is based on a mechanically pumped fluid loop with parallel tubes carrying coolant to reject heat from the radiator surface. A series of valves actuate to start and stop fluid flow to different combinations of tubes, in order to vary the heat rejection capability of the radiator by a factor of 10 or more. When the flow in a particular leg is stopped, the fluid temperature drops and the fluid can freeze, causing damage or preventing flow from restarting. For this reason, the liquid in a stopped leg must be partially or fully evacuated upon shutdown.

One of the challenges facing fluid evacuation from closed tubes arises from the vapor generated during pumping to low pressure, which can cause pump cavitation and incomplete evacuation. Here we present a series of laboratory experiments demonstrating fluid evacuation techniques to overcome these challenges by applying heat and pumping to partial vacuum. Also presented are results from qualitative testing of the freezing characteristics of several different candidate fluids, which demonstrate significant differences in freezing properties, and give insight to the evacuation process.

Nomenclature

C_p	=	specific heat
E	=	energy
L	=	latent heat of vaporization
M	=	molar mass
m	=	mass
P	=	pressure
PGW	=	propylene glycol/ water mixture
R	=	universal gas constant
T	=	temperature
V	=	volume

¹Member of Technical Staff, Thermal Hardware and Fluid Systems Engineering Group, 4800 Oak Grove Drive, Pasadena, California 91109, AIAA Member.

²Principal Engineer, Thermal and Cryogenic Engineering Section, 4800 Oak Grove Drive, Pasadena, California 91109, AIAA Member.

³Associate Member of Engineering Staff, Thermal Hardware and Fluid Systems Engineering Group, 4800 Oak Grove Drive, Pasadena, California 91109, AIAA Member.

⁴Senior Member of Engineering Staff, Thermal Hardware and Fluid Systems Engineering Group, 4800 Oak Grove Drive, Pasadena, California 91109.

⁵Group Supervisor, Thermal Hardware and Fluid Systems Engineering Group, 4800 Oak Grove Drive, Pasadena, California 91109, AIAA Member.

⁶Project Manager Advanced Thermal Technology Project, Exploration Technology Development Program, Houston, Texas 77058. AIAA Member.

⁷Undergraduate Student, 344 S. Latah #201 Boise, ID 83705

I. Introduction

The design of future human-rated spaceflight missions will strive for lightweight, efficient systems to push the boundaries on what is currently possible. Future human missions to near-Earth objects, the moon, or Mars will likely encounter more extreme hot and cold thermal environments than previous missions^{1,2}. For thermal management systems, this drives the need for research into new and innovative system architectures. Unlike robotic missions that can utilize low-freeze-point coolants^{3,4}, human spaceflight demands stringent control of the environment experienced by the delicate human body, with minimal risk of exposure to toxic chemicals or extreme temperatures. Traditional thermal management systems for human missions utilize a dual-loop pumped fluid system, with one loop circulating fluid within the warm cabin environment, and the other transporting fluid to a cold radiator^{5,6}. This architecture allows the use of a toxic working fluid with very low freeze temperature for the cold radiator section, and a non-toxic fluid for the warm environment near the astronauts. A heat exchanger transfers heat between the two loops, enabling cabin heat to be rejected to the radiator. Recent research has shown that a single-loop architecture can deliver a mass savings of 18%⁶, compared to the dual-loop system. This architecture brings a new challenge, however, as non-toxic fluids must be used, most of which have relatively high freeze temperatures.

Digital radiator technology is one of several promising emerging concepts currently under development to deliver a lightweight single-loop solution to meet the rigorous demands of human spaceflight missions⁷⁻⁹. The basic concept, shown schematically in Fig. 1, pumps working fluid from the warm spacecraft to a radiator, or a set of radiators, where the flow is distributed into several parallel lines. These lines are individually valved, allowing flow to be stopped and started at will to rapidly vary the heat rejection capability of the system. This allows for variation of the heat rejection by at least a factor of 10^{7-9} , and the rapid turn-down can ease the requirements for additional Supplemental Heat Rejection Devices (SHReDs), such as transient sublimators¹⁰, to handle large thermal transients. This is an advantage of the digital radiator over other variable radiator technologies, such as stagnation radiators, which cannot respond to rapid changes in environmental heating. Thus, while a digital radiator system without a SHReD must still be sized for the peak heat load for a particular mission, its ability to rapidly adjust can reduce the requirement for SHReDs, which must be present in other systems to respond to rapid variations.

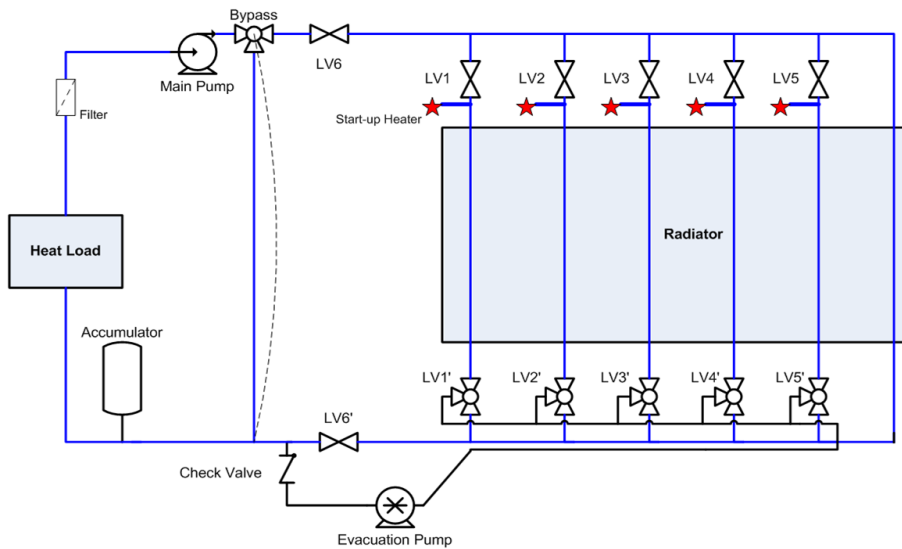


Figure 1. Digital Radiator Concept Schematic

The ability to rapidly vary the radiator heat rejection allows for highly flexible mission design over a wide range of thermal environments. This technology is not without challenges, which must be overcome to demonstrate its usefulness for flight systems. The primary challenge involves freezing of fluid in stopped lines that are exposed to cold temperatures. Because of the single-loop architecture, the working fluid may encounter temperatures well below the freezing point when flow in a line is stopped. This fluid must therefore be evacuated from all stopped lines to prevent freezing and allow restart. Furthermore, the behavior of these fluids is not well characterized near the freeze point, making modeling difficult.

The remainder of this document will be divided into two parts. The first part will cover a series of experiments

qualitatively investigating the freezing behavior of several candidate working fluids for use with the digital radiator and other thermal management technologies for human space missions. The second part will detail experimental work for fluid evacuation of lines in the digital radiator, addressing design challenges and mitigation strategies.

II. Fluid Freezing Experiments

This series of experiments was intended to investigate qualitatively the nature of the freezing process of several candidate fluids for human-rated missions. This study was initially motivated by the ambiguity of fluid thermal data from manufacturers, and disagreement between data from different sources. Additionally, disagreement between modeled and experimental results by the stagnation and freezable radiator teams¹¹ demonstrated the need for experiments to give insight to the physical nature of the freezing process for these fluids. This information will also help define requirements for digital radiator designs for specific missions, in terms of the need to evacuate tubes to avoid freezing vs. allowing cold flow. As the results below will show, the different fluids demonstrate substantially different freezing behavior from one another.

Table 1 lists the fluids tested, along with their approximate “freeze” temperatures from the literature. For fluids without a distinct phase change, the term “pour point” refers to the temperature below which the fluid will no longer freely flow when poured from an open vessel¹². This term is often imprecisely defined and used interchangeably with the term “freeze point.”

Table 1. Published fluid freeze temperatures

Fluid	Freeze T (°C)
Qtherm SZ2	-50
Multi-Therm WB-58	< -62
Galden HT-170	-97 (pour)
Propylene Glycol (pure)	-57 (pour)
PGW (50/50)	-34 (pour)

Figure 2 shows a photograph of the experimental setup for the freeze tests. A copper cup contains the fluid, which also has a removable lid not shown in the photograph. A recirculating-fluid chiller provides cooling by pumping a separate coolant fluid (Syltherm XLT) through copper coils, which are soldered to the outside of the cup. This chiller has a minimum set point of -60°C, which provides a minimum wall temperature of the inside wall of the cup of -57°C. For testing of fluids with freeze points near or below this temperature, the chiller can be replaced with a liquid nitrogen feed line to achieve cryogenic temperatures. The copper cup rests atop a magnetic stir plate, which provides an optional means to agitate the fluid during the early stages of freezing. A clear polycarbonate enclosure surrounds the experiment, and a gaseous nitrogen purge line fills this box with dry gas to preclude any condensation or deposition of moisture or condensable gases into the experimental fluids or onto cold surfaces.

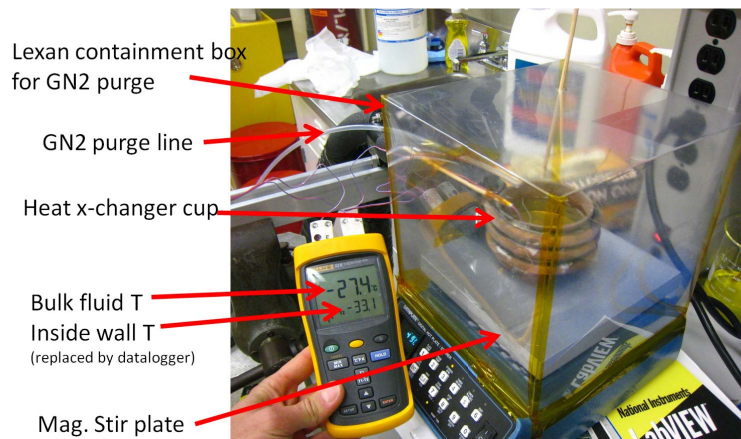


Figure 2. Fluid freeze test setup photograph

Two thermocouples provide temperature data: one in contact with the inner wall of the cup below the fluid level, and the other immersed in the bulk liquid. The photograph shows a hand-held readout for the thermocouples, but this was replaced by a computer data acquisition system for automated data logging. This, and a concentration measurement described later, provide the only quantitative data for these freezing experiments.

A. Propylene Glycol/ Water

The baseline fluid for a proposed manned lunar mission consists of a 50/50 mixture (by weight) of propylene glycol and water (PGW). For this reason, we studied this fluid most extensively in the freeze experiments. Figure 3 shows a series of photographs during a freezing sequence of PGW, with no stirring, along with temperatures from the bulk and wall thermocouples for each image. The photographs proceed sequentially in time from left to right, starting at the top left. In this image, roughly hexagonal clumps of opaque material form and grow from unseen nucleation sites on the bottom and walls of the container. Upon later stirring of this mixture using a manual stirring rod, the translucent portion of the mixture proved to be highly viscous liquid, similar to honey. The opaque material was not a hard solid, but rather a soft, putty-like material that could be easily deformed, but was significantly closer to solid than the clear portion.

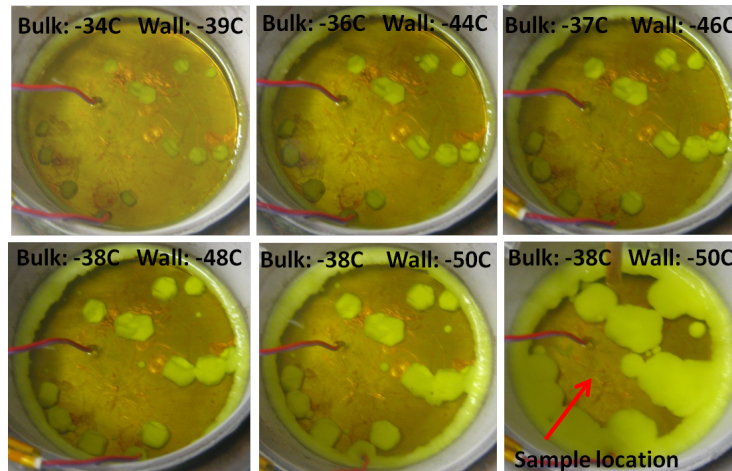


Figure 3. PGW unstirred freezing progression

Figure 4 shows a plot of the wall and bulk fluid temperatures vs. time from the two thermocouples in the system. The oscillations in wall temperature are caused by imperfect feedback control of the temperature control system in the chiller and represent real variations of a few degrees. This plot shows a gradual decrease of the bulk fluid temperature as time progresses, with no distinct plateaus indicative of a “classic” phase change. This shows the gradual nature of PGW freezing with a poorly defined freeze temperature.

During another test, the magnetic stirrer agitated the mixture until the viscosity increased to the point at which it could no longer move freely, after which a manual rod hand stirrer was used through a small hole in the plastic enclosure. This test showed the appearance of white tendrils of material that grew and multiplied as the temperature dropped until the entire mixture became thick and opaque. Figure 5 shows a photograph of the thick PGW on a stirring rod at -57°C . This test, and the unstirred test, show a gradual phase change from liquid to solid, without a clearly defined freeze temperature.

After the unstirred freezing of the PGW mixture shown in Fig. 3, before manual stirring, a sample of the clear portion of the liquid was obtained for concentration analysis. This concentration analysis was performed by Andre Yavrouian at JPL using a Karl Fisher Titrator. The analysis was performed both for the sample taken after freezing, as well as a sample of the liquid before freezing to represent the original concentration for comparison. The results show negligible change of the relative concentrations of propylene glycol and water between the original and frozen samples. This indicates that the water does not preferentially freeze out of solution before the propylene glycol, but rather that the mixture maintains the original concentration throughout the freezing process.

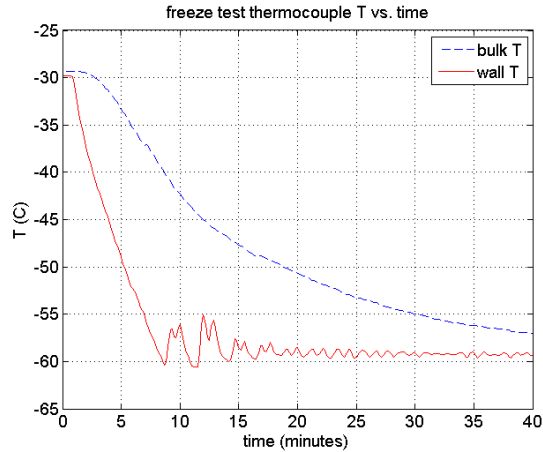


Figure 4. Plot of thermocouple data for unstirred PGW cooling showing no distinct phase-change plateau



Figure 5. PGW mixture after cooling to bulk $T=-57^{\circ}\text{C}$

B. Qtherm SZ2

The Qtherm SZ2 showed significantly different freezing behavior than the PGW mixture. This fluid, a mixture of salts dissolved in water, showed a much more distinct phase change than the PGW. Figure 6 shows a sequence of images from a non-stirred freezing test, similar to those shown for the PGW. The fluid becomes opaque long before the freeze temperature is reached, and long before the viscosity increases significantly. Upon freezing, the fluid becomes a coarse, “snow-cone-like” loosely bonded solid below -26°C . This is in sharp contrast to the published data, which gives a freeze temperature of -50°C . Figure 7 shows a plot of the bulk liquid thermocouple temperature vs. time for a freeze test, which shows a distinct plateau around -26°C , indicating a classic phase change.

C. Galden HT-170

Galden HT-170 has a pour point of -97°C , as listed by the manufacturer, and was therefore tested using single-pass liquid nitrogen in place of the recirculating chiller. During the freeze test, the fluid remained translucent, and formed a hard solid layer on the walls and bottom of the copper cup. Figure 8 shows an image sequence for this freeze test. This hard layer became cracked as it thickened, in a manner similar to water ice upon freezing in a constraining vessel. Before freezing into a hard layer, the fluid became gradually more viscous, reaching a consistency of honey before becoming solid. According to the thermocouple data, shown in Fig. 9, no distinct phase change occurs. This is consistent with the literature, which lists a pour point rather than a freeze point for the fluid. The sharp downward spikes seen in the bulk temperature curve in Fig. 9 occur during manual stirring of the fluid, as colder fluid is transported from near the wall to the bulk thermocouple location.

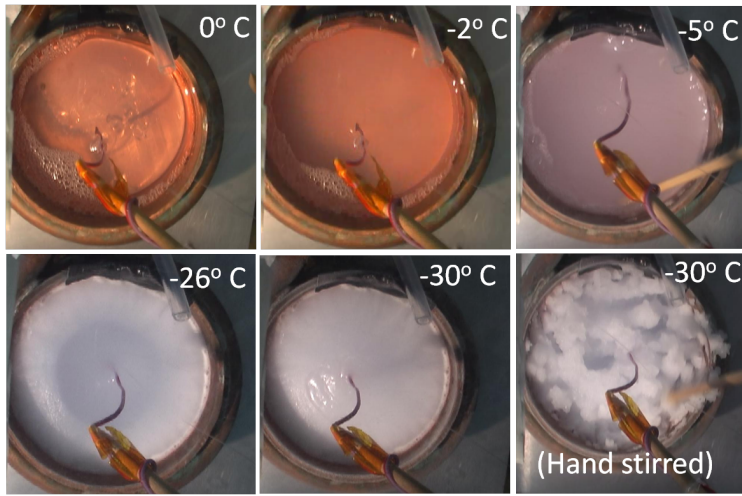


Figure 6. Freezing progression photographs for Qtherm SZ2

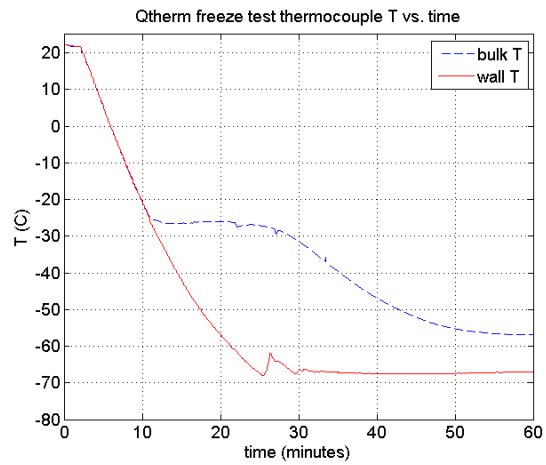


Figure 7. Plot of thermocouple temperature evolution for Qtherm SZ2



Figure 8. Galden freeze photo progression

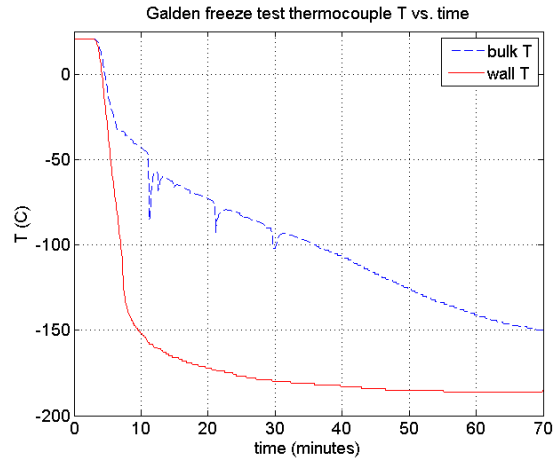


Figure 9. Plot of thermocouple temperature evolution for Galden HT-170

D. Multi-Therm WB-58

Multi-Therm WB-58 also tolerates very low temperatures and was tested using the liquid nitrogen setup. This fluid displayed qualitative properties somewhere between those of Galden and PGW, with an indistinct phase change gradually moving from liquid to a hard solid below -105°C . The bulk temperature plot shown in Fig. 10 lacks the distinct plateau of a well-defined phase change, but shows a noticeable change in slope and concavity around -70°C . This indicates some sort of phase change, more well defined than PGW, but less so than Galden HT-170.

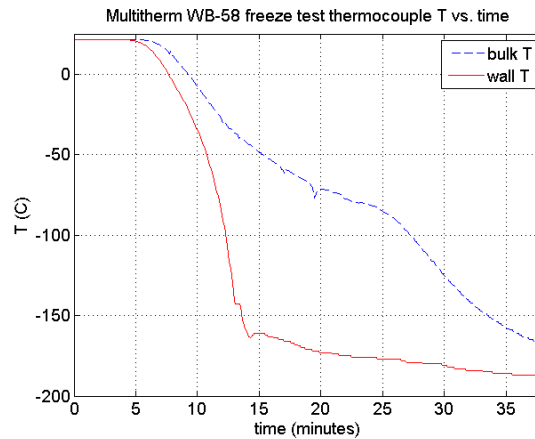


Figure 10. Plot of Multi-Therm WB-58 temperature evolution

E. Fluid Testing Discussion

This series of simple fluid freezing experiments highlights the substantial differences in freezing characteristics of the different candidate fluids. The tests furthermore show the nature of fluids with a poorly defined freezing point and gradual phase change. This indistinct phase change likely leads to the difficulties in accurately modeling flow of such fluids at cold temperatures. Modeling efforts for this and other radiator technologies, such as stagnation and freezable radiators, will require highly accurate data on fluid viscosity, specific heat, and thermal conductivity as a function of temperature^{11,13}. Furthermore, reproducibility of these properties after multiple freeze/thaw cycles must be evaluated. This was only done for two freeze/thaw cycles for PGW in our experiments (with nearly identical results). Testing to better quantify these properties by performing more detailed testing has recently been initiated under the direction of personnel at Johnson Space Center^{14,15}.

For the purposes of the digital radiator technology, use of a fluid with ill-defined properties near the freezing point necessitates that the fluid not approach this temperature regime, for fear that the fluid may become excessively viscous or develop a hard layer on the wall to restrict flow to the point of stagnation. This condition may make re-warming or restarting flow impossible without the use of large amounts of heater power to melt the frozen fluid. This drives the requirement that tubes with stopped flow must be evacuated sufficiently so as to ensure a clear path with no blockage for restarting flow.

III. Fluid Line Evacuation Experiments

This section describes a set of experiments to reliably evacuate fluid from tubes and demonstrate the capability to chill and restart flow in cold, evacuated tubes. Prior experiments tested several different concepts for evacuating fluid. These included bubble injection, dissolved CO₂, fluid venting to space, use of surrogate tubes, and use of startup heaters⁸. The startup heater concept shows the most promise in terms of functionality, lightweight design, and mission flexibility, and is therefore the only concept carried forward for the additional testing presented here.

The startup heater concept uses a mechanical pump to draw a vacuum at the downstream end of the tube to be evacuated. A heater mounted inside of a “stub” leg at the upstream end warms the fluid to encourage boiling at the upstream end. This raises the local pressure upstream, so that a pressure gradient forms to drive the liquid towards the pump at the downstream end. The result is a vapor bubble that forms upstream and displaces the liquid as it grows in the downstream direction, filling the tube with vapor. The stub leg exists to provide a small reservoir of stagnant liquid that can boil to provide a continuous source of vapor formation for the evacuation of long tubes. The stub leg is not part of the radiator flow path, and freezing of any remaining liquid in the stub will not impede the flow of fluid to restart flow to evacuated legs. Figure 1 shows a schematic of the digital radiator system with the stub leg heater concept, and Figure 11 shows the schematic for the laboratory evacuation experiment setup.

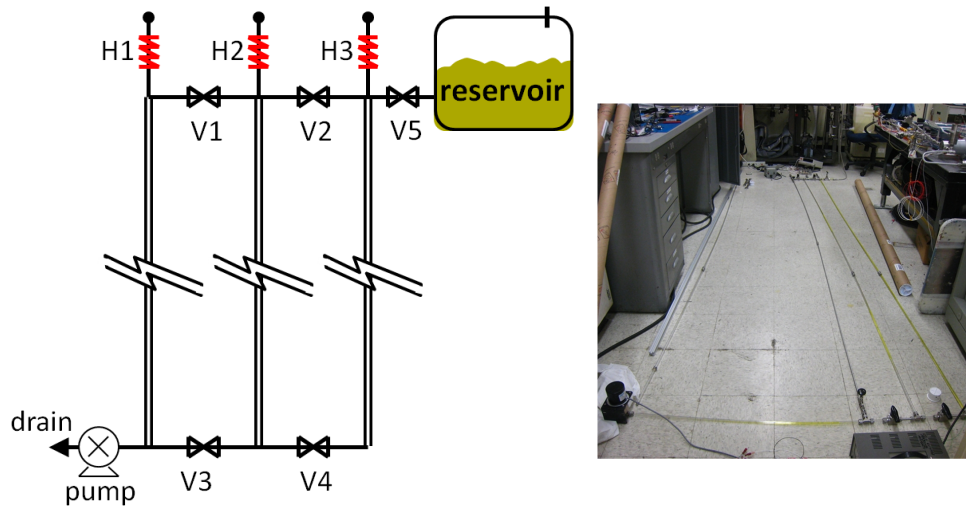


Figure 11. Experimental setup schematic (L) and photograph (R) for tube evacuation testing

A. Theory

The theoretical amount of energy that must be transferred into the liquid to generate sufficient vapor to displace liquid from the entire tube can be calculated as the latent heat of vaporization plus the energy required to raise the appropriate mass of liquid to the boiling point.

$$E = L \cdot m_{boiled} + m_{heated} \int C_p \cdot dT \quad (1)$$

Here, m_{boiled} is the mass of liquid actually vaporized, m_{heated} is the mass of liquid heated to near the boiling point, L is the latent heat of vaporization, and C_p is the specific heat of the liquid. From reference¹⁶, L for 50% PGW is 1.57×10^6

J/kg, and C_p is estimated as an approximately linear function of temperature:

$$C_p[J/kg \cdot K] = 5.85T[K] + 2390 \quad (2)$$

For the minimum theoretical energy, the mass of liquid heated is equal to the mass of liquid vaporized to fill the entire tube volume (V) with vapor. This mass can be calculated using the ideal gas law:

$$P \cdot V = m(R/M)T \quad (3)$$

Here, R is the universal gas constant and M is the molar mass of PGW ($M=47 \text{ g/mole}$)¹⁶. We consistently measured a pressure (P) of approximately 0.5 psia (3400 N/m^2) at the downstream end of the tube during evacuation. At this pressure, the boiling point is approximately 61°C ,¹⁶ and we assume a starting temperature of 10°C (the minimum radiator outlet temperature). For a 3/8in. x 12ft. ($9.5\text{mm} \times 3.7\text{m}$) evacuated tube, this gives a total energy input of approximately 70 J.

For a more realistic estimation, however, we must consider that the heat cannot practically be delivered exclusively to the small mass of liquid to be boiled. A finite amount of liquid will invariably be heated and not boiled, requiring additional energy input to the system. Also, more liquid must be boiled to account for re-condensation at the colder downstream regions. Additionally, some waste heat will flow into the metal tube and surroundings. Assuming that this waste heat can be minimized by careful design and thermal insulation, we consider only the additional energy required to heat the volume of liquid surrounding the heater element to near the boiling point. For our laboratory experiment, we use a stub leg of 1/2in. (12.7mm) outer diameter tubing, and a 2in. (50.8mm) long immersed heater element. Assuming that the liquid in this cylindrical volume is heated from 10°C to near 61°C , the total energy requirement for single tube evacuation becomes approximately 1200 J. This demonstrates the need for heater/ stub leg design optimization before the development of a flight-like system.

B. Smooth-Wall Tube Experiments

These tests demonstrate evacuation of multiple full length (12ft.) tubes, according to the full scale digital radiator design.^{8,9} Figure 11 shows the experimental setup. Manual valves are denoted V1, V2, etc., and heaters are denoted H1, etc. Fluid leg numbers are called out by the number of the associated heater. All of the evacuation tests presented here utilize immersion cartridge-style heaters, mounted in a fitting at the end of a stub leg so as to lie in the center of the tube as shown in Fig. 12. Comparison to prior testing with external film heaters applied to the outer tube surface showed the immersion heaters to be more effective at quickly delivering heat to the fluid with less waste to the surrounding metal. Tests with 1/8in. (3.2mm), 1/4in. (6.4mm), and 3/8in. (9.5mm) diameter heaters showed the 1/8in. heaters to be most efficient in terms of total energy required for tube evacuation. However, these small heaters were easily damaged by overheating. A flight-like design would likely employ a temperature feedback circuit to control the heater temperature and allow the use of the most efficient design possible. For the sake of robust laboratory testing we use the 1/4in. x 2in. heaters unless otherwise noted.



Figure 12. Photograph of stub heater in fitting

The fluid used for all tests is the baseline PGW 50/50 mix (Amsoil ANT¹⁷). A positive-displacement mechanical gear pump provides the suction for evacuation. Most of these tests use 3/8in. O.D. translucent polycarbonate tubing, unless otherwise noted, in order to enable flow visualization for qualitative performance evaluation.

The final digital radiator design will use aluminum tubing, which will likely have somewhat different surface properties than polycarbonate. However, a simple test shows that polycarbonate has similar static liquid-solid surface tension as aluminum. In this test, a drop of PGW was placed on a flat, horizontal surface of various materials. The droplet on the surface was photographed edge-on using a digital camera, and the contact angle at the droplet edge was measured from the photographs. Figure 13 shows these photographs and contact angles for several materials, showing

that polycarbonate and aluminum have similar contact angles with PGW. While far from a rigorous test of the surface-liquid interaction properties, this encourages the use of polycarbonate tubing for early testing of flow visualization. As we will later show, the two materials demonstrate similar tube evacuation performance.

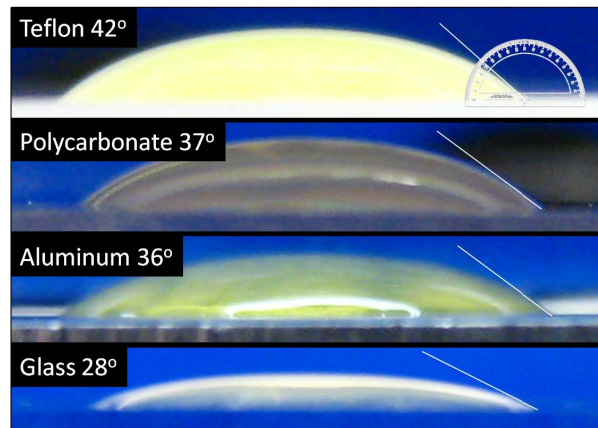


Figure 13. PGW droplet contact angle on various surfaces

C. Three Tube Evacuation Testing

These experiments tested the feasibility of evacuating multiple tubes using a single heater, multiple heaters in parallel evacuation, and multiple heaters with series evacuation. For the single heater with multiple tubes test, V1, V2, V3, and V4 were opened, and only heater H3 operated at power levels ranging from 20W to 100W. Operation of H1 or H2 in place of H3 was tested also with similar results. With this configuration, evacuation of all three tubes was not possible. In all tests, one tube evacuated before the others. When this occurs, a clear path forms for vapor to flow from the heater to the pump. This short-circuits the flow path, diminishing the pressure gradient necessary to evacuate liquid from the other two tubes. Thus it is necessary for each tube to be isolated from the others on the upstream end, and for each tube to have its own heater.

For the parallel evacuation experiments, V1 and V2 were closed, and V3 and V4 remained open. All three heaters operated simultaneously at 35W each for 110s, and the pump operated for 3 minutes. With this configuration, we were able to achieve full apparent evacuation in all three tubes. However, the evacuation was not reliable, often leaving significant slugs of liquid. The evacuation proceeded very slowly, likely limited by the speed of the pump when pulling fluid from three parallel legs. This slow evacuation resulted in random boiling of the liquid, creating vapor pockets which caused the pump to operate at a lower pressure differential than when pulling a solid liquid column.

Evacuation of tubes in series proved to be the most reliable. In these tests, V1 and V2 were closed for the duration. V3 and V4 began open and H3 was energized for 90s, and the pump operated for 2 minutes for reliable evacuation. After leg 3 evacuated, V4 was closed and H2 energized for similar time scale. After leg 2 was evacuated, V3 was closed and H1 energized. This method results in reliable apparent full evacuation of all three tubes, but requires 5-6 minutes of total pump run time.

In all of these experiments, we use the term “apparent full evacuation” to denote evacuation of a clear polycarbonate tube to the point where no liquid can be seen. In all of these cases of apparent evacuation, however, we observed the post-evacuation appearance of small “slugs” of liquid, as shown in the photograph in Fig. 14. These slugs appear on a time scale of several minutes after evacuation, and are formed from the thin film of liquid remaining adhered to the tube walls. After several minutes, surface tension forces (in the absence of inertial forces) cause the annular liquid film to coalesce into liquid slugs filling the tube cross section.¹⁸ For all tests, the remaining liquid amounts to approximately 15% of the total evacuated volume. Further testing of evacuation by opening the upstream end to atmosphere (causing very rapid evacuation in a few seconds) showed similar results of remaining liquid. These slugs pose a risk of flow blockage upon freezing. The last part of this section describes the use of internally finned tubing to mitigate the blockage.

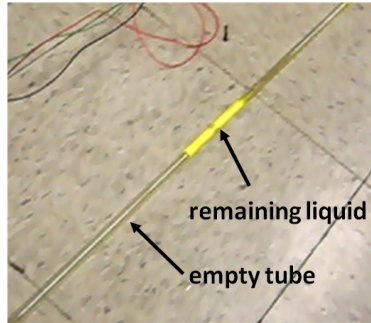


Figure 14. Photograph showing remaining liquid slugs after post-evacuation coalescence

D. Single Line Gravity Tests

These tests use only one tube of the three tube setup, with V1 and V3 closed to isolate the leg attached to heater H1. The tube is mounted to a stiff aluminum beam with either end elevated to create an incline or decline with respect to the gravity vector. Three cases were tested with this configuration, plus one without the beam:

1. Decline with upstream end elevated by 1.4in. (36mm) (0.5° decline)
2. Incline with downstream end elevated by 1.4in. (36mm) (0.5° incline)
3. Incline with downstream end elevated by 5.3in. (135mm) (2° incline)
4. Both ends elevated by 1.4in. and sagging in the middle (beam not used)

All four cases achieved apparent full evacuation with similar heater powers and evacuation times as the flat cases. However, the observation of fluid coagulation into slugs after evacuation was significantly different for each case. For the decline case, the coalescing fluid moved to the downstream end and eventually was removed by briefly re-energizing the heater and pump. For both inclined cases, the fluid coalesced preferentially near the upstream end. Upon re-energizing the heater and pump, a small amount of fluid was removed but most was lost to the walls: as the fluid slug moved downstream it visibly shrank until very little remained at the pump. For the case with both ends elevated, the fluid quickly coalesced into slugs in the low middle portion immediately after evacuation, while the pump was still running. At this point, the slugs quickly moved downstream and approximately half of the remaining fluid passed through the pump and out of the system. However, there still remained a small slug of fluid which could block the flow upon freezing. Furthermore, a spacecraft system clearly cannot rely upon a gravity effect for proper operation.

Additional testing of aluminum single line tubes in a horizontal orientation verified the existence of roughly 15% remaining fluid after evacuation of $\frac{1}{4}$ in. and $\frac{3}{8}$ in. aluminum tubes. The effect of post-freeze flow blockage in these tubes was also confirmed by cooling the tubes to approximately -55°C , after which fluid could not flow until the tubes were warmed.

E. Internally Finned Tubing Experiment

To mitigate the problem of post-evacuation liquid slug formation and subsequent flow blockage, this experiment used $\frac{3}{8}$ in. O.D. aluminum tubes with axial fins on the interior walls, as shown in the photograph of the tube section in Fig. 15. This tubing was originally developed for heat pipe construction for use on the Mars Science Laboratory.¹⁹ The narrow channels between the fins trap excess fluid in the tube and spread it axially by means of capillary forces, thus preventing the liquid from coalescing into slugs. With this fin design, the total inter-fin channel volume accounts for approximately 30% of the total internal tube volume, providing sufficient space to trap the excess 15% of un-evacuated liquid.

Figure 16 shows the experimental setup used to test the finned tubing concept. Three $\frac{3}{8}$ in. x 12ft. (9.5mm x 3.7m) tubes, one finned and two smooth, are bonded together in a triangular formation to create similar thermal contact between all three. The finned tube and one smooth tube serve as the evacuation test lines, and the second smooth tube connects to the recirculating chiller to flow coolant to cool the test lines. Foam insulation surrounds the entire assembly. One test line at a time can be installed in place of leg 1 in the previous experimental setup with V1 and V3 closed. An additional valve, hereby referred to as V6, is installed just upstream of the pump, in order to isolate

the test line after evacuation. The segments of tubing between the test line and V6, and between V6 and the pump remain clear polycarbonate for flow visualization.



Figure 15. Finned tubing section

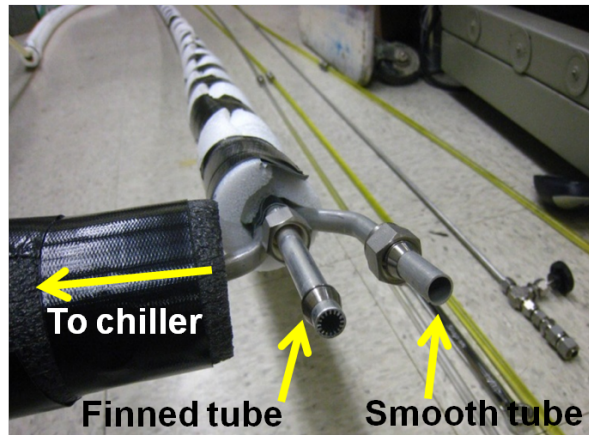


Figure 16. Finned tubing evacuation experiment setup

The experiment proceeded by first evacuating the finned test line by operating H1 at 35W for 90s and running the pump for 120s. After this, V6 was closed to isolate the line and the chiller was operated at -55°C for 4 hours. After chilling, the pump was restarted and V1, V2, V5, and V6 opened. Flow restarted immediately as seen in the clear downstream lines. Repetition of this procedure using the smooth-walled test line resulted in zero flow until the tube warmed sufficiently, which occurred roughly 15 minutes after stopping the chiller. This entire experiment was repeated thrice, with identical results each time.

IV. Conclusion

We have demonstrated successful and reliable evacuation of full-scale-length tubes for the digital radiator concept, including multiple tube evacuation and restarting flow after chilling. The problem of post-evacuation liquid coalescence and subsequent tube blockage is effectively mitigated by the use of internally-finned tubing to trap and spread excess liquid. Testing continues at JPL to more thoroughly evaluate the startup heater as a viable option for a digital radiator design, as well as to optimize the heater/ tubing configuration for minimum energy consumption and maximum reliability. These tests will include evacuation of aluminum finned tubing of varying diameter, translucent finned tubing for flow visualization, and installation of heaters with built-in fins for trapping of liquid in the stub section. Also the testing will include more thorough systematic evaluation of different heater sizes and types to minimize power input and maximize evacuation reliability.

Qualitative freeze testing of several candidate working fluids demonstrate the striking differences in freezing behavior between fluids and give insight to the freezing process. These tests highlight the ill-defined properties of many

of the fluids near the freeze point and show the need for an accurate property database to properly model flow behavior at cold temperatures.

The digital radiator concept can provide an efficient and highly flexible means of thermal management for spacecraft that experience drastically varying heat loads and thermal environments. The experiments presented here encourage further development of this technology, which holds great promise for single-loop architecture thermal management for future human space missions.

Acknowledgments

The research was carried out at the Jet Propulsion Laboratory, California Institute of Technology, under a contract with the National Aeronautics and Space Administration. The authors express their thanks to Ronald Reeve, Manager, Spacecraft Propulsion Technology (4132), Space Exploration Technology Program for his support and encouragement for this task.

References

- ¹Stephan, R., "Overview of NASA's Thermal Control System Development for Exploration Projects," AIAA International Conference on Environmental Systems, 2010-6135, July 2010.
- ²Stephan, R., "Overview of the Altair Lunar Lander Thermal Control System Design," AIAA International Conference on Environmental Systems, 2010-6080, July 2010.
- ³Birur, G. C., Bhandari, P., "Mars Pathfinder Active Heat Rejection System: Successful Flight Demonstration of a Mechanically Pumped Cooling Loop," SAE International Conference on Environmental Systems, 981684, 1997.
- ⁴Swanson, T. D., Birur, G. C., "NASA thermal control technologies for robotic spacecraft," Applied Thermal Engineering, Vol 23, Issue 9, June 2003, pp 1055-1065.
- ⁵Diamant, B. L., Humphries, W. R., "Past and Present Environmental Control and Life Support Systems on Manned Spacecraft," SAE International Conference on Environmental Systems, 901210, July 1990.
- ⁶Ochoa, D. A., Ewert, M., "A Comparison Between One- and Two-Loop ATCS Architectures Proposed for CEV," SAE International Conference on Environmental Systems, 09ICES-0353, July 2009.
- ⁷Ganapathi, G. B., Sunada, E. T., Birur, G. C., Miller, J. R., Stephan, R., "Design Description and Initial Characterization Testing of an Active Heat Rejection Radiator with Digital turn-down Capability," SAE International Conference on Environmental Systems, 2009-01-2419, July 2009.
- ⁸Sunada, E., Birur, G. C., Ganapathi, G. B., Miller, J. R., Berisford, D. F., Stephan, R., "Design and Testing of an Active Heat Rejection Radiator with Digital Turn-Down Capability," AIAA International Conference on Environmental Systems, 2010-6159, July 2010.
- ⁹Miller, J. R., Birur, G. C., Ganapathi, G. B., Sunada, E. T., Berisford, D. F., Stephan, R., "Design and Modeling of a Radiator with Digital Turn-Down Capability under Variable Heat Rejection Requirements," accepted for publication in AIAA International Conference on Environmental Systems, July 2011.
- ¹⁰Sheth, R., Leimkuehler, T., Stephan, R., "Investigation of Transient Performance for a Sublimator," AIAA International Conference on Environmental Systems, AIAA-2010-6081, July 2010.
- ¹¹Navarro, M., "Assessment of a Freezable Radiator for Variable Heat Rejection," ESCG-4470-10-TEAN-DOC-0067, ESCG, June 4, 2010.
- ¹²ASTM D5853 - 09 "Standard Test Method for Pour Point of Crude Oils," ASTM Volume 05.01, Petroleum Products and Lubricants (I): D56 - D3710, February 2011.
- ¹³Iacomini, C., Linrud, C., Dang, J., Bailey, C., and Anderson, G., "Tube Stagnation Experiments and Modeling Using a Safe, Non-Corrosive Dielectric Fluid for Radiator Thermal Control Systems Near Stagnation Regimes," SAE International Conference on Environmental Systems, 08ICES-0228, July 2008.
- ¹⁴Lillibridge, S. T., "Freezable Radiator Test Report," CTSD-ADV-743, CTSD, January 27, 2011.
- ¹⁵Navarro, M., "Freezable radiator fluid candidate study," ESCG-4470-10-TEAN-DOC-0155, ESCG, September 28, 2010.
- ¹⁶The Dow Chemical Company, "A Guide to Glycols," Form Number: 117-01682-0804XSI, 2003 http://www.dow.com/PublishedLiterature/dh_02aa/09002f13802aaf25.pdf
- ¹⁷<http://www.amsoil.com/storefront/ant.aspx>
- ¹⁸Bousman, W. S., McQuillen, J. B., Witte, L. C., "Gas-Liquid Flow Patterns in Microgravity: Effects of Tube Diameter, Liquid Viscosity, and Surface Tension," Int. J. Multiphase Flow, Vol. 2, no. 6, pp. 1035-1053, 1996.
- ¹⁹Bhandari, P., Birur, G., Karlmann, P., Bame, D., Liu, Y., Mastropietro, A. J., Miller, J., Pauken, M., Ganapathi, G., Krylo, R., Kinter, B., "Mars Science Laboratory Mechanically Pumped Fluid Loop for Thermal Control – Design, Implementation, and Testing," SAE International Conference on Environmental Systems, 2009-01-2437, July 2009.